

# Liesegang patterns: Effect of dissociation of the invading electrolyte

B. Chopard<sup>1</sup>, M. Droz<sup>2</sup>, J. Magnin<sup>2</sup>, Z. Rácz<sup>3</sup>, and M. Zrinyi<sup>4</sup>

<sup>1</sup> *Département d'Informatique, University of Geneva, CH-1211 Genève 4, Switzerland*

<sup>2</sup> *Département de Physique Théorique, Université de Genève, CH 1211 Genève 4, Switzerland.*

<sup>3</sup> *Institute for Theoretical Physics, Eötvös University, 1088 Budapest, Puskin u. 5-7, Hungary*

<sup>4</sup> *Department of Physical Chemistry, Technical University of Budapest, H-1521 Budapest, Hungary*  
(September 29, 1998)

The effect of dissociation of the invading electrolyte on the formation of Liesegang bands is investigated. We find, using organic compounds with known dissociation constants, that the spacing coefficient,  $1 + p$ , that characterizes the position of the  $n$ -th band as  $x_n \sim (1 + p)^n$ , decreases with increasing dissociation constant,  $K_d$ . Theoretical arguments are developed to explain these experimental findings and to calculate explicitly the  $K_d$  dependence of  $1 + p$ .

## I. INTRODUCTION

Liesegang patterns are quasi-periodic structures precipitated in the wake of a moving reaction front. Although they appear only in specific physico-chemical conditions, these structures are widespread in nature and can be found in systems ranging from biological (populations of bacteria) to geological (structures in agate rocks) [1,2]. Depending on the geometry and the dimensionality of the system, the observed patterns are bands, rings or spheres, although it is also possible to generate more particular patterns such as spirals.

In chemistry, such structures are produced by allowing two chemicals, called  $A$  and  $B$ , initially separated, to mix through diffusion. The two components are chosen so that they react and form a nonsoluble product, called precipitate. In a typical example,  $B$  (the inner electrolyte) is initially dissolved in a gel and placed in a test tube. At time  $t = 0$ , the reagent  $A$  (outer electrolyte) is poured into the tube and it starts to diffuse into the gel. As the result of chemical and physical mechanisms such as nucleation, aggregation, coagulation or flocculation, opaque or colored zones called Liesegang structures are formed as the diffusive front of  $A$  moves ahead (see Fig.1 for an example).

The precipitation zones that appear in the tube usually exhibit a few well defined features. In particular, the time of the formation of the  $n$ -th band,  $t_n$ , and the distance of the  $n$ -th band from the initial interface,  $x_n$ , are related by the so called *time law* [3]:

$$x_n \sim \sqrt{t_n} \quad (1)$$

This law follows evidently from the diffusive nature of the reaction-diffusion front.

A more intricate property of the positions of the bands is that they usually form a geometric series,  $x_n \sim (1+p)^n$ , implying that  $x_{n+1}/x_n$ , tends to a constant for large  $n$ . This experimental observation is usually referred to as the *Jablczynski law* or *spacing law* [4]:

$$\frac{x_{n+1}}{x_n} \equiv 1 + p_n \xrightarrow{n \gg 1} 1 + p \quad (2)$$

The quantity  $1 + p$  will hereafter be referred to as the *spacing coefficient*. Usually  $p > 0$  and one speaks of regular banding.

A central goal of the studies of Liesegang bands is to understand how the spacing coefficient depends on both the experimentally controllable parameters (such as the initial concentrations of  $A$  and  $B$ ) and the other less controllable material parameters such as the diffusion coefficients. A major achievement from experimental point of view has been the establishment of the so called Matalon-Packter law [5,6]. It gives the dependence of the spacing coefficient on the initial concentration,  $a_0$ , of the outer electrolyte,  $A$ , in a simple form

$$1 + p = Q_1 + \frac{Q_2}{a_0}, \quad (3)$$

where  $Q_1$  and  $Q_2$  depend on the initial concentration,  $b_0$ , of the inner electrolyte as well as on all the other material parameters.

As far as the theoretical approaches are concerned, several competing theories have been developed [7–18], many of which [7–14] fare well in deriving the time and spacing laws [19]. They succeed in explaining the formation of these bands by following how the diffusive reagents  $A$  and  $B$  turn into immobile precipitate  $D$



taking into account various scenarios for the intermediate steps denoted here by  $\dots C \dots$ . The theories are not entirely equivalent when they are applied to derive the Matalon-Packter law and comparison with experiments slightly favors the so called *induced sol-coagulation* model [20]. It should be emphasized, however, that there is no clear experimental evidence at present that would distinguish decisively among the existing theories. Accordingly, it remains to be a task to search for distinguishing features of Liesegang phenomena both in experiments and theories.

From a chemical point of view the process given by (4) often means oversimplification. In some cases, for example, the precipitate  $D$  may partly redissolve in the surplus of component  $A$ . This is not a negligible effect since the precipitation and dissolution processes, coupled to diffusion, may lead to a propagating band instead of a final static pattern [21].

Another effect, that is our main concern in this paper, is the dissociation of the invading electrolyte  $A$ . In the theoretical approaches formulated up to now, it is usually assumed that the concentration of the reacting ions is equal to the concentration of the electrolyte. This is true only when an ionic compound, a strong acid or a strong base is used as  $A$ . If, however, a weak acid or weak base is used as outer electrolyte, then the two concentrations are not equal and the effect of dissociation must be taken into account.

As an explicit example, imagine the formation of  $Mg(OH)_2$  precipitate (this process will be our main concern throughout this paper). Consider a gel soaked with

$MgCl_2$ , and let us pour either  $NaOH$  or  $NH_4OH$  onto its surface. In both cases the chemistry is the same:  $Mg(OH)_2$  precipitate is formed. There are, however, significant differences in the patterns formed as shown in Fig.1. The strong base ( $NaOH$ ) results in a very dense band structure, whereas the weak base ( $NH_4OH$ ) produces a rather loose pattern. A more precise analysis reveals (see below) that the latter structure has a significantly larger spacing coefficient. Based on this example, one can conclude that either the co-ions or the different degree of dissociation have a strong influence on the final pattern. In previous experiments on Liesegang phenomena, we found that the effects of co-ions (such as  $Na^+$  or  $NH_4^+$ ) is almost negligible [22]. We shall therefore assume that the decisive role is played by the dissociation and that it may be possible to isolate the effect of dissociation on the formation of Liesegang bands. Since we aim at studying this effect and since we count physicists in our audience, a few words are in order about dissociation.

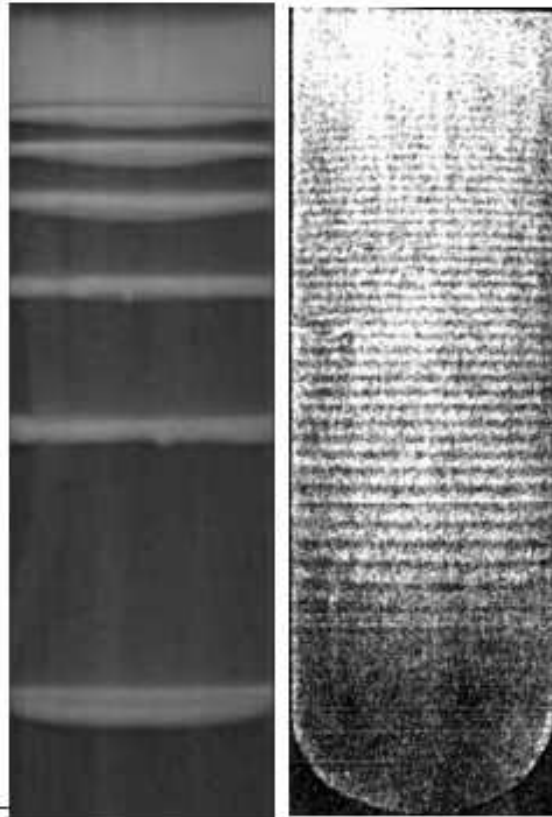
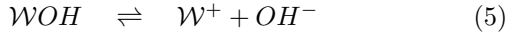


FIG. 1.  $Mg(OH)_2$  Liesegang patterns formed from the reaction of the inner electrolyte  $MgCl_2$  with two different outer electrolytes:  $NH_4OH$  for the left picture and  $NaOH$  for the right one.

Dissociation is a common phenomenon for acids and bases. Strong acids and bases dissociate into ions entirely i.e. the solution contains only ions but no neutral molecules. For weak acids and bases the dissociation is not complete and the neutral molecules and ions keep a

dynamical equilibrium in the solution.

In order to introduce notation, let us consider a weak base  $WOH$ . In an aqueous solution, the base, its cations,  $W^+$ , and anions,  $OH^-$ , are all present



and the equilibrium concentrations are related by

$$K_d = \frac{[W^+][OH^-]}{[WOH]} \quad (6)$$

where  $K_d$  is the *dissociation constant*. It is convenient to introduce the degree of dissociation,  $\alpha$  defined as

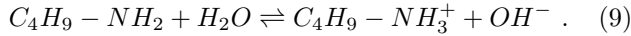
$$\alpha = \frac{[W^+]}{a_0} = \frac{[OH^-]}{a_0} \quad (7)$$

where  $a_0$  denotes the initial concentration of the base,  $a_0 = [WOH]_{t=0}$ . Then eq.(6) can be written as

$$K_d = a_0 \frac{\alpha^2}{1 - \alpha} \quad (8)$$

and one can see that  $\alpha$  can be determined once  $a_0$  and  $K_d$  are known.

In order to study the effect of dissociation on Liesegang pattern formed by  $Mg(OH)_2$  precipitate, several bases having different values of  $K_d$  are required. Unfortunately, there are only few inorganic ones available. Consequently, we have chosen organic compounds to provide the necessary  $OH^-$  ions. The organic molecules we shall use dissociate like the 1-buthylamin:



For our purposes, an important characteristic of an amine is its basicity that is conveniently expressed by the  $pK_a$  of its conjugate acid. For the sake of simplicity, however, we shall characterize the dissociation ability of amines by the basicity constant  $pK_b = 14 - pK_a$  that can be expressed through  $K_d$  as

$$pK_b = -\log(K_d/e_0) \quad (10)$$

where  $e_0 = 1\text{mol/dm}^3$  and  $K_d$  is given by eq. (8). The basicity constant is essentially a measure of an amine's ability to accept a proton from water according to (9). The higher the  $pK_b$  of an amine the lower is its dissociation ability.

The goal of this work can be now stated more precisely. We carry out a combined experimental and theoretical study of the effect of dissociation on the Liesegang patterns by investigating the  $pK_b$ -dependence of the spacing coefficient  $1 + p$ .

The paper is organized as follows. In Sec.2, we describe the experimental procedures and present the experimental data. The main finding here is that increasing the dissociation constant results in a decreasing spacing coefficient. In Sec.3, the theoretical models developed for explaining the formation of Liesegang patterns are generalized by including the dissociation effects. Then the spacing coefficient as a function of the dissociation constant is calculated explicitly and comparison with the experimental data follows. The conclusion is that all theoretical models that produce the Matalon-Packter law should be in qualitative agreement with the experiments.

## II. EXPERIMENTAL PART

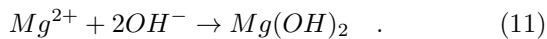
### A. Materials

We have studied the formation of  $Mg(OH)_2$  precipitate, by diffusion of inorganic and organic compounds into chemically cross-linked polyvinylalcohol (PVA) hydrogel containing the  $MgCl_2$  inner electrolyte.

Outer electrolyte	$pK_b$	$1 + p$
$NH_4OH$	4.75	$1.76 \pm 0.05$
2-buthylamine	3.44	$1.13 \pm 0.01$
i-propylamine	3.40	$1.110 \pm 0.005$
1,2-ethyldiamine	3.29	$1.09 \pm 0.01$
1-buthylamine	3.23	$1.09 \pm 0.01$
piperidine	2.88	$1.043 \pm 0.004$
NaOH	$-\infty$	$1.00 \pm 0.01$

Table I. Outer electrolytes, their basicity constants, and the corresponding spacing coefficients obtained from the experiments. Note that the case of  $NaOH$  appears to be special in that  $x_{n+1}/x_n \rightarrow 1$  for large  $n$  and the asymptotic form of  $x_n$  should be different from  $x_n \sim (1 + p)^n$ .

Table I lists the bases used for producing the ions  $OH^-$  as well as their basicity constants [23]. When the spatially separated reactants come into contact, the white precipitate  $Mg(OH)_2$  is formed as a result of the following reaction:



### B. PVA gels as reaction-diffusion media

The highly swollen PVA-hydrogels were prepared by cross-linking of primary PVA-chains with glutaric aldehyde (GDA) in aqueous solution, containing dissolved

$MgCl_2$ . Commercial PVA (Merck 821038) and solution of 25 mass% GDA (Merck) were used for preparation. The initial polymer concentration, as well as the cross-linking density has been kept constant. The polymer content of the PVA gels was in every case 3.5 mass%. The ratio of monomer unit of PVA (VA) to the cross-linking agent, GDA was:  $(VA)/(GDA) = 250$ . In order to study the precipitation and band formation in swollen networks, one of the reactants, the inner electrolyte  $MgCl_2$  was mixed with the polymer solution containing the cross-linking agent. The concentration of  $MgCl_2$  in the gel phase was constant ( $0.05 \text{ mol/dm}^3$ ). The gelation was induced by decreasing the pH of the system by  $HCl$  (Reanal, Hungary). Then the solution was poured into glass tubes. The gelling process usually took 3-4 hours. Experiments were made in tubes of length 300 mm and diameter 12 mm. The tubes were sealed and allowed to stand undisturbed at constant temperature of  $17^\circ C$ . After completion of the network formation, the outer reactants were brought into contact with the gels, so that they start to diffuse into it. The diffusion took place vertically downward at controlled temperature. We maintained the constancy of boundary condition by re-

freshing the upper solution continuously, thereby keeping the concentration of the outer electrolyte at a fixed value ( $7 \text{ mol/l}$ ). During all the experiment process, constant temperature of  $17.00 \pm 0.02^\circ C$  was maintained and the tubes were kept free from mechanical disturbances such as vibrations.

### C. Liesegang band formation

The penetration of organic as well as inorganic molecules into the gel containing the  $Mg^{2+}$  ions resulted in precipitate bands (see Fig. 1) with a sharp interfaces of  $Mg(OH)_2$ . In order to determine the position of bands we used a digital video system. A CCD camera with an  $1/3''$  video chip has been connected to a PC through a real-time video digitizer card. We have also used a scanner to digitalize the experimental results. We have determined the coordinate of the gel surface where the diffusion started. Then the position of the  $n$ -th band,  $x_n$ , was measured as the distance between the surface of the gel and the upper side of the  $n$ -th precipitate.

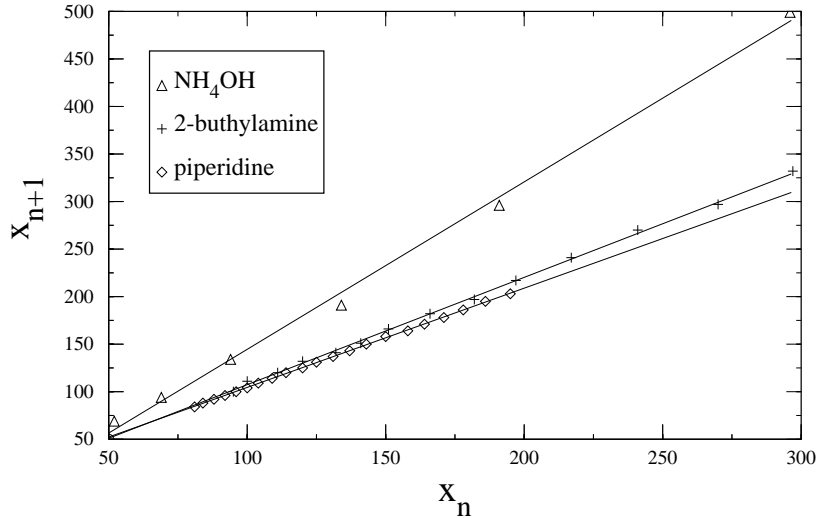


FIG. 2. Determination of the spacing coefficient given by slope of the curves  $x_{n+1}$  vs.  $x_n$  for different compounds. The distances are measured in pixels of the digitalized pictures. The choice of the unit length is irrelevant as we are interested in the ratio  $x_{n+1}/x_n$ . The straight lines are least-square fits.

In order to determine the value of the spacing coefficient we plotted  $x_{n+1}$  against  $x_n$ . For the sake of a better visibility, only three samples are shown on Fig. 2 but the other sets of data are of similar quality. The data were analyzed by linear least square method and the resulting spacing coefficients and related errors are summarized in Table I. Note that the relatively large number of bands

allowed a rather accurate determination of the spacing coefficients (of course, one should keep in mind that the errors quoted in Table I are the statistical errors and they do not include possible systematic errors).

The  $pK_b$  dependence of the spacing coefficient is shown in Fig. 3. One can easily see that increasing the dissociation ( $pK_b = 10^{-K_d}$ ) decreases the spacing coefficient. It

should be pointed out, however, that in contrast to the theories discussed below, where all parameters except  $K_d$  can be kept fixed, the situation is more complex in the experiments. All the parameters such as reaction thresholds and diffusion constants may, in principle, change when going from one outer electrolyte to the other. Thus

Fig.3 displays the coupling between the spacing coefficient and the value of  $pK_b$  under the assumption that one can neglect the effect of the co-ions on the material parameters that are relevant in the process of pattern formation.

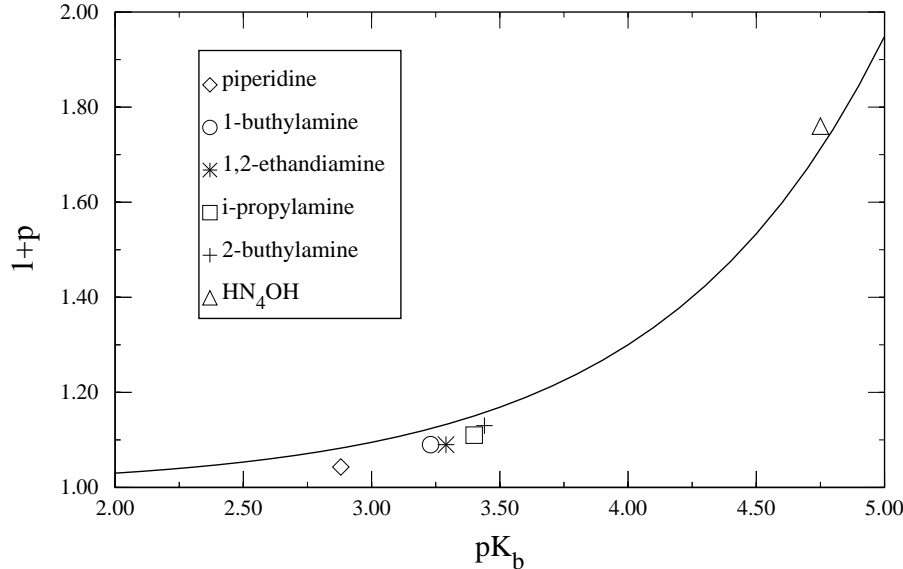


FIG. 3. Spacing coefficient  $1+p$  as a function of the basicity  $pK_b$  of the invading electrolytes. The full line is the prediction of the theory, eq.(22), with parameters  $Q_1 = 1$  and  $Q_2 = 0.003$ .

### III. THEORETICAL APPROACHES

The formation of precipitation bands is a rather complex phenomenon and it is by no means certain that there exist a unified description of all Liesegang phenomena. Indeed, several theories have been developed. All of them follow how the diffusive reagents  $A$  and  $B$  turn into immobile precipitate  $D$  through some intermediate steps  $A + B \rightarrow \dots C \dots \rightarrow D$ . The common feature of the theories is that the precipitate appears as the system goes through some supersaturation and nucleation thresholds. The differences arise in the details of treating the thresholds and in the growth kinetics of the precipitate.

Our aim here is not to review these theories in detail (a recent critical discussion can be found in [20]). Instead, we shall recall them briefly, highlight their specific features and then discuss how dissociation enters into the problem. We shall see that the experimentally relevant regime of dissociation that is fast compared to diffusional relaxation, can be treated independently of the details of the theories. The final result is that, since the Matalon-Packter follows from all of the theories, the consequence of the dissociation is universal. Namely, the spacing co-

efficient depends exponentially on the basicity constant,  $pK_b$ .

#### A. Supersaturation of ion-product theory

The simplest theory is based on the concept of *supersaturation of ion-product* [7] and has been developed by many researchers [8–10,24]. In this theory, the  $A, B$  reagents turn into the precipitate  $D$  (without any intermediate steps) provided the local product of concentrations of the reactants,  $ab$ , reaches some critical value,  $q^*$ . The nucleated particles grow, deplete  $A$  and  $B$  in their surroundings and, as a consequence, nucleation stops. When the reaction zone (where  $ab$  is maximum) moves far enough so that the depletion effect of the precipitate becomes weak, then  $ab = q^*$  is reached again and nucleation can occur. This quasiperiodic process leads to the formation of successive bands. In the limit of very large precipitation- and aggregation rates, the control parameters of this model are the initial densities of the electrolytes  $a_0$  and  $b_0$ , their diffusion coefficients  $D_a$  and  $D_b$  and the ion-product threshold  $q^*$  [20].

## B. Nucleation-and-growth theory

The *nucleation-and-growth theory* introduces a single intermediate step in  $\dots C \dots$  with a mechanism of band formation based on the supersaturation of the intermediate compound  $C$  [13,14]. In this theory,  $A$  and  $B$  react to produce a new diffusing species  $C$  the nature of which is not really specified. It may be a molecule as well as a colloid particle. The main event is the nucleation that occurs when the local concentration of  $C$ -s reaches some threshold value. The nucleated particles ( $D$ -s) act as aggregation seeds and the nearby  $C$ -s aggregate to the existing droplet (hence become  $D$ -s) provided their local concentration is larger than a given aggregation threshold. These models are characterized by two thresholds,  $c^*$  for nucleation and  $g^*$  for droplet growth. As before,  $a_0, b_0, D_a, D_b$  are control parameters but the diffusion constant  $D_c$  of the  $C$  species and  $c^*, g^*$  appear as extra control-parameters [20]. The depletion mechanism around an existing precipitation band is similar to the one described for the ion-product theory and it leads to the quasiperiodic band formation.

## C. Induced sol-coagulation theory

The nucleation-and-growth theories have been modified to take into account effects of the concentration of the electrolytes on the nucleation processes. In the *induced sol-coagulation* theory [11,12], it is assumed that  $A$  and  $B$  react to produce a sol ( $C$ ) and this sol coagulates if both the concentration of  $C$  exceeds a supersaturation threshold  $c \geq c^*$  and the local concentration of the outer electrolyte is also above a threshold  $a > a^*$ . The quantity  $a^*$  is often referred to as the *critical coagulation concentration threshold* and is a new free parameter in this theory. The band formation is a consequence of the nucleation and growth of the precipitate combined with the motion of the front where  $a = a^*$ .

## D. Reaction-diffusion equations

All the above theories can be described in terms of reaction diffusion equations for the concentrations of the reagents ( $a, b, c$ ) and of the precipitate ( $d$ ):

$$\partial_t a = D_a \partial_x^2 a - R_1(a, b, c, d), \quad (12)$$

$$\partial_t b = D_b \partial_x^2 b - R_1(a, b, c, d), \quad (13)$$

$$\partial_t c = D_c \partial_x^2 c + R_2(a, b, c, d), \quad (14)$$

$$\partial_t d = R_3(a, b, c, d). \quad (15)$$

where the reaction terms  $R_\alpha$  can always be chosen so that they describe the precipitation and aggregation processes which are building blocks of the theories discussed above. The time- and the spacing laws (1,2) follow from

the equations corresponding to the above theories. Furthermore, using these theories, one can also derive [20] the experimentally observed Matalon-Packter law (3),  $1+p = Q_1 + Q_2/a_0$ . This is an important law because  $a_0$  is one of the few experimentally controllable parameter in Liesegang phenomena. As we shall see, the knowledge of the simple  $a_0$  dependence of  $1+p$  allows us to derive the effects of the dissociation on the spacing coefficient.

## E. Role of dissociation

The outer electrolyte  $A$  produces the reagent  $\bar{A}$  through reversible dissociation  $A \leftrightarrow \bar{A} + A'$ . This process of dissociation can be characterized by a relaxation time,  $\tau_{dis}$ , defined as the typical time taken by a molecule to dissociate and thus to equilibrate the local ionic concentrations. This is a *microscopic* time and thus it should be much smaller than the time of diffusional relaxation of density profiles. Indeed, the diffusive front of the  $A$  particles moves with a velocity  $v_f \sim \sqrt{D_a/t}$  that diminishes with time. Thus the relaxation time of density perturbations over a characteristic distance  $\ell$  ( $\ell$  can be the width of the reaction zone,  $w \sim t^{1/6}$  [25], or the distance between consecutive bands  $x_{n+1} - x_n \sim \sqrt{t_n}$ ) increases without bound i.e. it is a *macroscopic* time

$$\tau_{diff} \sim \frac{\ell}{v_f} \sim t^\sigma, \quad \sigma \geq 1/2. \quad (16)$$

Consequently, in the long time limit,  $\tau_{dis}$  becomes negligible and we can assume the existence of a *local dissociation equilibrium*. Thus we can extend relation (6) to the out-of-equilibrium situation, where concentrations depend on  $x$  and  $t$ . This implies that, denoting the density of the reagent ion of the outer electrolyte  $\bar{A}$  by  $\bar{a}$ , the first reaction diffusion equation (12) must be replaced by the following couple of equations:

$$\partial_t a = D_a \partial_x^2 a - \kappa_1 a + \kappa_2 \bar{a}^2 \quad (17)$$

$$\partial_t \bar{a} = D_{\bar{a}} \partial_x^2 \bar{a} + \kappa_1 a - \kappa_2 \bar{a}^2 - R_1(\bar{a}, b, c, d). \quad (18)$$

where  $\kappa_1, \kappa_2 \rightarrow \infty$  accounting for  $\tau_{dis} \gg \tau_{diff}$  and  $\kappa_1/\kappa_2 = K_d$  ensuring that the steady, homogeneous state satisfies the steady state condition (6). The rest of the equations (13,14,15) change only by  $a \rightarrow \bar{a}$  in the reaction terms.

Equations (17,18) together with the rest of the reaction-diffusion equations (13,14,15) can be solved numerically and the spacing coefficient can be determined within the framework of the various theories. We do not have to carry out this work, however, since the concentration of the outer electrolyte in a usual experimental setup is two orders of magnitude larger than that of the inner electrolyte. This means that, for practical purposes, the precipitation processes do not influence the concentration profile of  $A$ . In turn, this means that the concentration of  $\bar{A}$  is determined by that of  $A$  and, using the fact that the local dissociation equilibrium is established fast, we

return to the original problem of equations (12,13,14,15) but with the initial concentration,  $a_0$ , replaced by  $\bar{a}_0$  as determined from the steady state condition, eq.(8):

$$\bar{a}_0 = \frac{K_d}{2} \left( \sqrt{1 + 4 \frac{a_0}{K_d}} - 1 \right). \quad (19)$$

It follows then that the effect of dissociation on the Matalon-Packter law can be obtained by just replacing  $a_0$  by  $\bar{a}_0$  in eq.(3):

$$1 + p = Q_1 + \frac{2Q_2}{\sqrt{K_d^2 + 4a_0K_d} - K_d} \quad (20)$$

$$= Q_1 + \frac{2 \cdot 10^{pK_b} Q_2 / e_0}{\sqrt{1 + 4 \cdot 10^{pK_b} a_0 / e_0} - 1}. \quad (21)$$

where we have replaced  $K_d$  by the experimentally measured basicity parameter  $pK_b = -\log(K_d/e_0)$  in the second equation. This expression of the spacing coefficient through the basicity parameter is the central result of our theoretical discussion. The derivation has no recourse to the details of the underlying theories of precipitation and so the result is valid for any theory that reproduces the Matalon-Packter law.

In the experiments discussed in previous chapters, the basicity parameter is large ( $pK_b \sim 3 - 5$ ) and since  $a_0 \approx 7e_0$ , we have  $10^{pK_b} a_0 / e_0 \gg 1$ . As a consequence, the Matalon-Packter law simplifies to

$$1 + p = Q_1 + \frac{Q_2}{\sqrt{a_0 e_0}} 10^{pK_b/2} \quad (22)$$

thus resulting in a simple exponential dependence on the basicity constant,  $pK_b$ .

## F. Comparison between experiments and theory

The functional forms obtained above (eqs.21,22) are universal in the sense that the  $pK_b$  dependence is explicit and only  $Q_1$  and  $Q_2$  depend on the details of the theories. Unfortunately,  $Q_1$  and  $Q_2$  contain unknown parameters such as aggregation thresholds and so they should be considered as fitting parameters. Nevertheless, it remains a question whether the experimental data could be fitted with reasonable values of  $Q_1$  and  $Q_2$  (the only obvious restriction on  $Q_1$  and  $Q_2$  coming from theories is that  $Q_1 \geq 1$  and  $Q_2 \geq 0$ ).

Fig.3 shows the experimental data together with the theoretical curve (22) using  $Q_1 = 1$  and  $Q_2 = 0.003$  and the agreement we see is very good. This is somewhat surprising. Indeed, using various outer electrolytes changes not only the dissociation constants but may alter the diffusion constants of the reagents ( $Mg^{2+}$ ,  $OH^-$ ) as well as it may change the various precipitation thresholds. The spacing coefficient should depend on all those quantities

and the surprise here is that these dependences are not significant or absent entirely. The agreement actually points to the correctness of our initial assumption that the  $Mg^{2+}$  and  $OH^-$  ions dominate the process with the co-ions playing no role at all except for the co-ion of  $OH^-$  setting the initial concentration of the  $OH^-$  ions.

As we can see, the above theoretical studies of dissociation and the comparison with experiments did not help in deciding which was the right theory for Liesegang phenomena. On the other hand, these studies lead to a simple picture of how the dissociation affects the spacing coefficient and, furthermore, it has been possible to express the results in simple analytical form that should be useful when discussing and designing Liesegang patterns.

## IV. SUMMARY

Our experiments show that the spacing coefficient of Liesegang patterns is strongly influenced by the degree of dissociation of the outer electrolyte. The dependence of  $1 + p$  on the basicity constant,  $pK_b$  has been found to be exponential and this experimental finding has been explained on the basis of the present theories of Liesegang phenomena.

## ACKNOWLEDGMENTS

We thank T. Antal, P. Hantz, and T. Unger for useful discussions. This work has been partially supported by the Swiss National Science Foundation in the framework of the Cooperation in Science and Research with CEEC/NIS, by the Hungarian Academy of Sciences (Grant OTKA T 019451 and T 015754), and by the EP-SRC, United Kingdom (Grant No. GR/L58088).

- 
- [1] R.E. Liesegang, Naturwiss. Wochenschr. **11**, 353 (1896);
  - [2] H. K. Henisch, "Periodic precipitation", Pergamon Press, (1991).
  - [3] Harry W. Morse and George W. Pierce: *Diffusion and Supersaturation in Gelatine*, Proceedings of the American Academy of Arts and Sciences, **38** 625-647 (1903)
  - [4] K. Jablczyński, Bull. Soc. Chim. France **33**, 1592 (1923).
  - [5] R. Matalon and A. Packter, J. Colloid Sci. **10**, 46 (1955);
  - [6] A. Packter, Kolloid Zeitschrift **142**, 109 (1955).
  - [7] W. Ostwald, "Lehrbuch der allgemeinen Chemie", Engelmann ed., Leipzig (1897).
  - [8] C. Wagner, J. Colloid Sci., **5**, 85 (1950).
  - [9] S. Prager, J. Chem. Phys. **25**, 279 (1956).
  - [10] Ya .B. Zeldovitch, G.I. Barrenblatt and R.L. Salganik, Sov. Phys. Dokl. **6**, 869, (1962).

- [11] N.R. Dhar and A.C. Chatterji, *Kolloid-Zeitschrift* **37**, 2-9 (1925); *J. Phys. Chem.* **28**, 41-50 (1924).
- [12] S. Shinohara, *J. Phys. Soc. Japan* **29** 1073 (1970).
- [13] G.T. Dee, *Phys. Rev. Lett.* **57**, 275 (1986).
- [14] B. Chopard, P. Luthi and M. Droz, *Phys. Rev. Lett.* **72**, 1384 (1994); *J. Stat. Phys.* **76**, 661-676 (1994).
- [15] M. Flicker and J. Ross, *J. Chem. Phys.*, **60**, 3458-3465 (1974).
- [16] S. Kai, S. C. Müller, and J. Ross, *J. Chem. Phys.*, **76**, 1392 (1982).
- [17] R. Feeney, S.L. Schmidt, P. Strickholm, J. Chadam, and P. Ortoleva, *J. Chem. Phys.*, **78**, 1293 (1983).
- [18] G. Venzl, *J. Chem. Phys.*, **85** 1996, 2006 (1986).
- [19] There are theories [15–18] which attribute the formation of Liesegang bands to the postnucleation instability present in the coarsening process. These theories however fail in explaining the regularity of the band spacing.
- [20] T. Antal, M. Droz, J. Magnin, Z. Rácz and M. Zrinyi, *Derivation of the Matalon-Packter law for Liesegang patterns*, to appear in *J. Chem. Phys.*, dec. 1998 (available by ftp from jcp.uchicago.edu).
- [21] M. Zrinyi, L. Gálfi, É. Smidróczki, Z. Rácz, and F. Horkay, *J. Chem. Phys.* **95**, 1618 (1991).
- [22] É. Smidróczki, PhD thesis, Budapest (1996).
- [23] CRC Handbook of Chemistry and Physics, 75<sup>th</sup> edition, D.R. Lise, ed., CRC Press Boca Raton, Ann Arbor, London, Tokyo (1913-1995).
- [24] D. A. Smith, *J. Chem. Phys.* **81**, 3102 (1984).
- [25] L. Gálfi and Z. Rácz, *Phys. Rev.* **A38**, 3151 (1988).